



Title	Multilayer passive RF microfabrication using jet-printed Au nanoparticle ink and aerosol-deposited dielectric
Author(s)	Roberts, RC; Tien, NC
Citation	The 17th International Conference on Solid-State Sensors, Actuators and Microsystems (Transducers & Eurosensors XXVII), Barcelona, Spain, 16-20 June 2013. In Conference Proceedings, 2013, p. 178-181, no. M3P.042
Issued Date	2013
URL	http://hdl.handle.net/10722/189860
Rights	International Conference on Solid State Sensors and Actuators Proceedings. Copyright © IEEE.

MULTILAYER PASSIVE RF MICROFABRICATION USING JET-PRINTED AU NANOPARTICLE INK AND AEROSOL-DEPOSITED DIELECTRIC

R.C. Roberts and N.C. Tien*

Department of Electrical and Electronic Engineering, The University of Hong Kong, HONG KONG

ABSTRACT

We report a bi-material additive microfabrication technique combining inkjet-printed gold films and an aerosol-deposited dielectric enamel for the realization of multilayer microsystems. Hexanethiol-encapsulated gold nanoparticle ink enables metal deposition at atmospheric pressure with a maximum temperature of 200°C. Dielectric patterning is achieved via shadow mask. Process utility is demonstrated for passive radio frequency components through the realization of spiral inductors and resonant parallel L-C tanks. The resulting device parameters agree well with theory, and the resonators exhibited a Q of 60 at 596MHz, the highest quality factor of an as-printed ink-jet microfabricated gold resonant structure to date.

KEYWORDS

Additive Microfabrication, Inkjet printing, Gold Nanoparticles, Printed Resonator

INTRODUCTION

Surface micromachining using drop-on-demand inkjet printing is an emerging additive microfabrication technique for the realization of sensors and actuators through the selective deposition of material from a liquid precursor, or ink [1, 2]. Printed metal microfabrication offers promise of low-cost processing by minimizing material usage. Further, many metal inks can be deposited at low temperatures, enabling the use of large-area low-cost polymeric substrates. These inks typically consist of metal nanoparticles (NPs) suspended in a carrier solvent, and often use an organic encapsulant to achieve solubility. Post-deposition thermal steps are required to remove organics and sinter these NPs together.

In order to use inkjet-printing to fabricate multilayer geometries such as those found in microelectronics and microelectromechanical systems (MEMS), a process compatible structural dielectric material must be identified to complement the conductive layers. The material must have usable dielectric characteristics, while being thermally compatible with the process temperatures and durations required for device manufacturing. The material must also be stable when exposed to the potentially volatile carrier solvents present during inkjet deposition to which the dielectric material will be exposed during the deposition of subsequent layers.

Spray coating is a technique widely used in the surface finish and adhesive industries to conformally coat surfaces of arbitrary size and topology [3]. Aerosol-based spray coatings are widely used for industrial and consumer applications, including photoresists. The promise of conformal deposition on arbitrary substrates makes aerosol-deposited materials attractive for additive microfabrication, warranting further exploration.

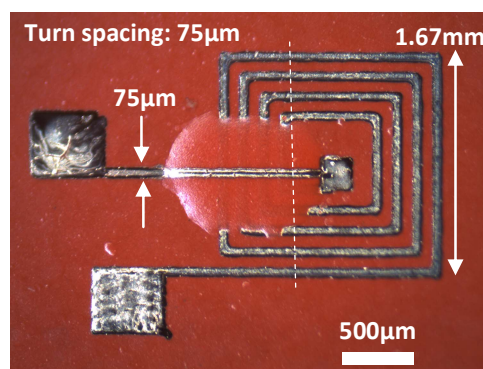


Figure 1: 24.0nH gold spiral inductor realized using this process flow. The dielectric bridge center height is 18µm.

Conventional microfabrication has found numerous applications in radio frequency (RF) systems including high-performance filters, phase shifters, low-loss switches, and as reactive components [4]. Currently, there is considerable interest for low-cost printed gold 13.56MHz RF identification (RFID) tags which have been reported with best as-printed Q of ~5, with a maximum Q of 30-100 using additional wet gold electroplating steps to reduce film resistivity [5]. Planar single-layer printed RF antennas and filters have also been realized on paper substrates using silver [6]. Just as conventional electronics created a strong demand for microfabricated RF components, the growing field of printed electronics will require process compatible multilayer RF devices.

This paper presents a hybrid multilayer additive microfabrication process using both inkjet-printed metal and aerosol-deposited dielectric. Inkjet printing allows for the patterning conducting layers with fine features. Dielectric passivation layers often do not require fine features, so a low-cost laser-cut polymer shadow mask is used to pattern the aerosol-deposited dielectric. Inkjet printing and shadow-masking are used in successive order to demonstrate multilayer microfabrication of passive RF components including the spiral inductor shown in Fig. 1.

MATERIAL SELECTION

Au Nanoparticle Ink

Gold (Au) is an attractive metal for microfabrication due its lack of a native oxide under ambient conditions. Therefore an Au ink comprised of hexanethiol-encapsulated gold nanoparticles (Au-NPs) suspended in α -terpineol, has been selected for this study. Recently, this material has been printed into pillars and patterned in microfluidic channels [7, 8], further demonstrating its utility for microfabrication. To realize coherent metal films from hexanethiol-encapsulated Au-NPs, post-deposition steps are required to sublimate the organics and sinter the Au-NPs together, as illustrated in Fig. 2. The Au-NP sintering process is monitored by measuring their conductivity during heating. A large decrease in

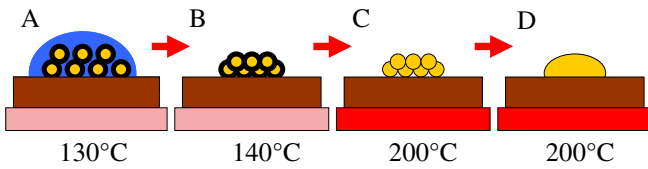


Figure 2: Ink Deposition Process: (A.) Au-NPs suspended in α -terpineol (blue) deposited onto heated substrate. (B.) Solvent evaporates. (C.) Temperature increased, sublimating the hexanethiol encapsulant (black). (D.) Au-NPs sinter together forming a coherent gold film.

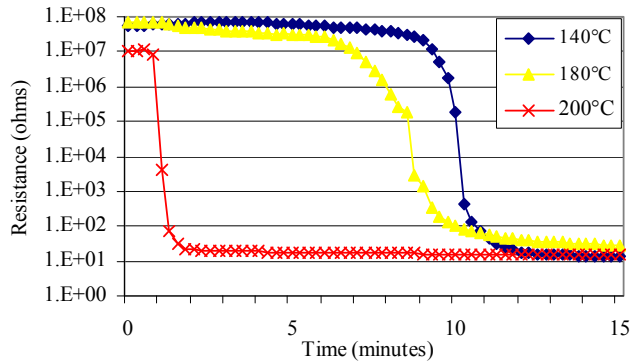


Figure 3: Resistance during sintering of 900 μ m long, 79 \pm 8 μ m Au-NP lines on Corning 0215 glass after 30 minute pre-bake at 140 $^{\circ}$ C on a hotplate in air. After 1 hour the line resistance of the three samples averaged 14.0 \pm 2.5 Ω -cm.

resistance is observed at the onset of sintering as shown in Fig. 3. Further synthesis and sintering details of the ink used herein are published elsewhere [9].

Aerosol Dielectric

Many aerosol-based dielectric materials on the market cannot handle the aggressive temperatures and solvents present during Au-NP inkjet printing. However, one suitable candidate identified is a high-temperature enamel formulated for aftermarket automotive engine applications. Manufactured by the Rust-Oleum Corporation and marketed as *Engine Enamel* (Part: 248941, Chevy Orange), this enamel has a glossy surface finish and is designed to be stable for temperatures up to 260 $^{\circ}$ C while resisting degradation when exposed to solvents. Due to the low-cost and ready availability of this aerosol-based dielectric, it was selected to demonstrate the prototype multilayer process.

FABRICATION PROCESS

The additive microfabrication process developed for this work is depicted in Fig. 4. In preparation, hexanethiol-encapsulated Au-NPs were first synthesized and suspended in α -terpineol (15%wt) to form a stable precursor ink. A custom inkjet deposition has been constructed using 30 μ m diameter piezoelectric nozzles (MicroFab, Inc.). The nozzle was driven with a 20Hz bipolar waveform using 2/5/2/5/2 μ s timing parameters at \pm 30V. Details of the printer and ink synthesis are located elsewhere [10]. Each Au-NP layer was printed using two consecutive passes onto a 130 $^{\circ}$ C platen. As the ink-jet parameters depend on the underlying surface properties, clean substrates were prepared by spray-coating Corning 215 glass with the aerosol-based dielectric enamel until

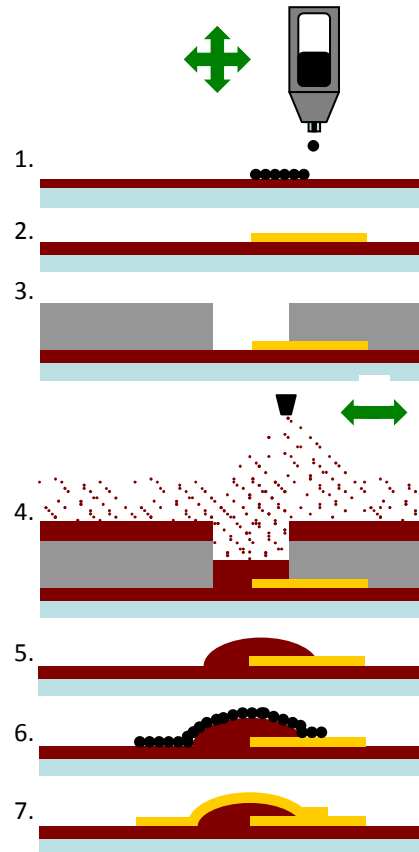


Figure 4: Process Flow: (1) Bottom Au layer printed, (2) Au-NP sintering, (3) Shadow mask applied, (4) Aerosol deposition of dielectric, (5) Mask removed, dielectric cured, (6) Top Au layer printed, (7) Top Au-NP sintering.

uniform visually. These air-dried for 30 minutes before transferring onto a hotplate at 200 $^{\circ}$ C for 1 hour yielding a thickness of 25 \pm 10 μ m. The bottom Au-NP was selectively jetted to pattern the bottom device layer and held at 140 $^{\circ}$ C for 30 minutes for solvent removal. Next, the substrate was heated to 200 $^{\circ}$ C for 1 hour on a hotplate to induce sintering, and then cooled to room temperature.

A shadow mask prepared from a 125 μ m thick polyester film (3M CG3700) and cut using a 50W CO2 laser cutter (Versalaser, Inc.) was then aligned onto the device. Enamel was then aerosol-deposited using a 1-2 second burst at a distance of 300mm. After a 5 minute air dry, the shadow mask was removed, and the device baked for 1 hour at 200 $^{\circ}$ C. Removal after 5 minutes allows the enamel to reflow, forming round edge suitable for printing. The dielectric is cured for 1 hour at 200 $^{\circ}$ C, and then the top gold layer inkjet deposited and sintered under identical conditions as the bottom gold layer to form the three layer topology explored in this work.

DEVICE DESIGN

Spiral Inductor

A 4-turn planar spiral inductor was selected at the first device to test hybrid microfabrication using a high-temperature dielectric enamel and inkjet printed gold nanoparticle ink due to their widespread use in RF integrated circuits. The relevant design parameters for this

device are shown on Fig. 1 and a predicted inductance of 23.8nH was computed using the Modified Wheeler approximation [11]. 500 μ m by 500 μ m pads were patterned at the end of each inductor trace to allow probing. A 400 by 750 μ m rectangular shadow mask was used to pattern the dielectric bridge.

LC Tank

The spiral inductor was then extended to include a discrete printed capacitor integrated in parallel to form an LC tank in an effort to build a structure similar to RF MEMS components and enabling the dimensions of either passive component to be resized independently for greater flexibility. As the resistance of the sintered Au films can be significant, an RL//C model was selected for parameters estimation, where a resistor and inductor are placed in series to a parallel capacitor [12]. In this configuration, the resonant frequency can be estimated as:

$$\omega_0 = \left(\frac{1}{LC} - \frac{R^2}{L^2} \right)^{\frac{1}{2}} \quad (1)$$

The LC tank consists of an identical 4-turn inductor with 840 μ m by 840 μ m square electrodes added both gold layers forming a parallel-plate capacitor using the enamel as the dielectric. The enamel shadow mask was cut to 1250 μ m by 1250 μ m for the capacitor region with a 200 μ m wide trace to the center of the inductor. The dielectric was oversized to ease alignment requirements and minimize edge effects.

RESULTS AND DISCUSSION

The 4-turn inductors were subsequently manufactured using the process outlined above with a 2 second dielectric deposition time. An optical micrograph of the realized 4-turn inductor is shown in Fig. 1, and a profilometry scan is displayed in Fig. 5. The four turns are apparent and the thick concave dielectric layer dominates the center of the cross section with the top gold trace visible at the top. The maximum dielectric bridge thickness was measured to be 18 μ m. Figure 6 details the sintered Au films on cured enamel using an SEM. The first gold layer appears to spread more than the second, and holes are observed in the film. The inductor was then characterized on a Karl Suss PM5 probe station using an Agilent E4980A LCR meter at 1MHz to have the following device parameters: $L_s=24.0\pm 0.1$ nH, and

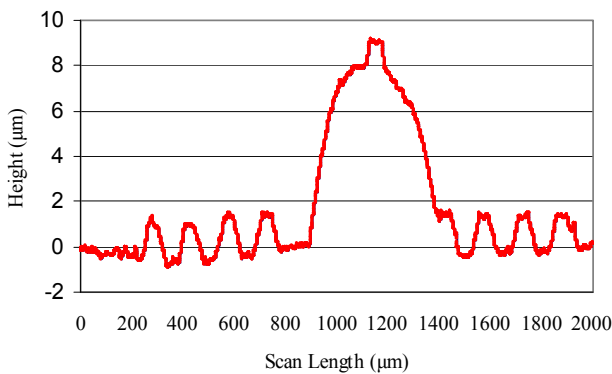


Figure 5: Stylus profilometer scan of the Fig. 1 inductor (dotted line). Au film thickness measured to be 1.9 μ m.

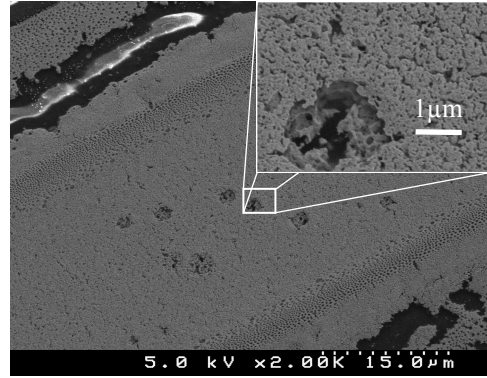


Figure 6: Scanning Electron Micrographs showing Au film detail of sintered Au-NP films onto aerosol-deposited enamel. Holes hypothesized to be due to solvent venting.

$R_s=63.3\pm 0.1\Omega$. The DC resistance of the coil was 65.5 $\pm 0.1\Omega$. The relative dielectric constant of the cured enamel was measured to be 3.1-3.2 from 1kHz-2MHz using the parallel plate capacitor technique.

Next, the LC tank devices were fabricated in a batch of six devices using the fabrication technique. The dielectric deposition time was reduced to 1 second. An optical micrograph of a realized device is shown in Fig. 7 with lateral dimensions shown. The dielectric on the inductor is a drop from shadow mask removal. Stylus profilometry was used to measure the topology of the parallel plate capacitor; the thickness of the dielectric measured between 6 μ m and 12 μ m with the maximum thickness in the center of the capacitor. Further improvements of this deposition technique are needed, as manual deposition is highly variable. Using the measured device parameters and (1), the expected resonance was estimated at 615MHz.

The LC tanks were then characterized using an Agilent 8720ES S-parameter analyzer on a Karl Suss PM-5 probe station. The test setup was first calibrated and configured for S12 parameter measurement. Figure 7 shows the characteristic frequency response of one LC Tank at resonance. The device operates at a resonant frequency of 596MHz, very close to the expected value. The quality factor of the resonator was computed by measuring the -3dB bandwidth and found to be 60. The resistance at resonance was computed as 210k Ω . Of the six devices fabricated during this run, three of them were electrically functional. Two devices suffered failures due

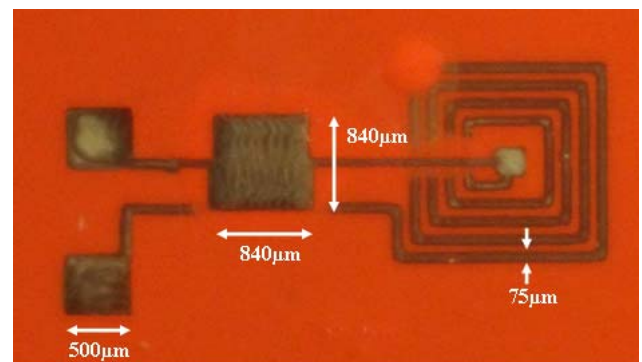


Figure 7: Resonant parallel L-C tank, using the inductor geometry from Fig. 1 and parallel plate capacitors, realized in this work.

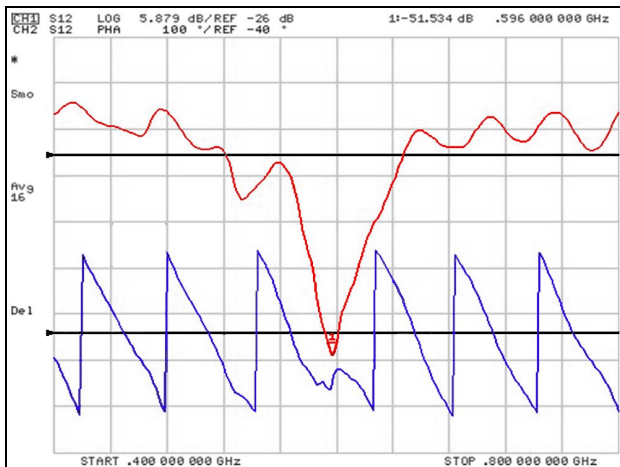


Figure 7: S_{12} measurements on an Agilent 8720ES of the LC tank with -20dB drive power, magnitude (top) and phase (bottom). The measurements reveal maximum Q of 60 at 596MHz for the printed LC tank.

to inconsistency of the dielectric deposition which can be solved through improved deposition equipment and masking techniques. The third device failed due to a break in the trace connecting the top gold trace to the bottom gold layer, likely due to stresses from thermal cycling. In order to improve dielectric uniformity and repeatability, the aerosol-deposition process should be automated. Alternatively, the liquid enamel precursor is a viable candidate for inkjet deposition directly.

CONCLUSIONS

A prototype additive micromachining process using inkjet-printed gold and the aerosol-deposited enamel as both the base substrate and interlayer dielectric has been demonstrated, enabling the realization of multilayer systems. All conducting gold layers were deposited via inkjet printing from a hexanethiol-encapsulated gold nanoparticle ink and subsequently sintered in air. The dielectric enamel was found to be promising as both an insulating and surface passivation layer, but large thickness variation due to the manual aerosol-deposition and shadow masking techniques should be improved.

Using this process an inkjet-printed gold inductor using the dielectric enamel as both the base substrate and the dielectric bridge was demonstrated and performed as predicted with a measured inductance of $24.0 \pm 0.1\text{nH}$ at 1MHz. This process was then further extended to realize the first inkjet printed gold parallel LC tank using discrete a discrete inductor and capacitor which was characterized and found to have a resonant frequency of 596MHz and a Q of 60. This performance compares favorably to other printed resonators in the literature including a 150MHz silver nanoparticle resonant coil ($Q=20$) [1]. Printed gold 13.56MHz RFID tags have been demonstrated ($Q=30-100$), but gold electroplating was used to improve the best as-printed performance ($Q \sim 5$) [5]. In comparison, the device realized using the process techniques developed in this work represents the highest Q of an *as-printed* LC resonant tank using sintered inkjet-printed Au-NPs.

This work has introduced a novel additive microfabrication process using an aerosol-deposited

dielectric material and inkjet-printed gold to fabricate passive RF components. Further refinement of the aerosol-deposition technique or developing the enamel as a jettable material is required in the future to improve the capabilities of this additive microfabrication process and allow the realization of more complex geometries. Further, exploration of a larger number of device layers is warranted.

REFERENCES

- [1] S. Fuller, E.J. Wilhelm, and J.M. Jacobson, "Ink-Jet Printed Nanoparticle Microelectromechanical Systems," *J. Microelectromech. Syst.*, 11 (54), pp. 54-60, 2002.
- [2] E.W. Lam, H. Li, and M.A. Schmidt, "Silver Nanoparticle Structures Realized By Digital Surface Micromachining," *Transducers 2009. Intl. Conf. on*, pp. 1698-1701, 2009.
- [3] H. Chen, W. Sheng, N. Xi, M. Song, and Y. Chen, "Automated robot trajectory planning for spray painting of free-form surfaces in automotive manufacturing," *Robotics and Automation, 2002. Proceedings. ICRA '02. IEEE Intl. Conf. on*, vol.1, pp. 450- 455, 2002
- [4] G. M. Rebeiz: "RF MEMS, Theory, Design and Technology," John Wiley & Sons, 2003.
- [5] V. Subramanian, J.M.J. Frechet, P.C. Chang, D.C. Huang, J.B. Lee, S.E. Molesa, A.R. Murphy, D.R. Redinger, and S.K. Volkman, "Progress Toward Development of All-Printed RFID Tags: Materials, Processes, and Devices," *Proc. of the IEEE*, vol.93, no.7, pp.1330-1338, July 2005
- [6] Li Yang; Rida, A.; Vyas, R.; Tentzeris, M.M.;, "RFID Tag and RF Structures on a Paper Substrate Using Inkjet-Printing Technology," *Microwave Theory and Techniques, IEEE Trans. on*, vol.55, no.12, pp.2894-2901, Dec. 2007
- [7] S.H. Ko, J. Chung, N. Hotz, K.H. Nam, and C.P. Grigoropoulos, "Metal nanoparticle direct inkjet printing for low-temperature 3D micrometal structure fabrication," *J. Micromechanics and Microengineering.*, 20, 125010, 2010.
- [8] M.T. Demko, J.C. Cheng, and A.P. Pisano, "High-resolution direct patterning of gold nanoparticles by the microfluidic molding process," *Langmuir*, 26 (22), 2010.
- [9] R.C. Roberts, and N.C. Tien "Thermoresistive Characteristics of Sintered Inkjet Printed Gold Nanoparticle Microstructures," *Technical Digest, The 11th IEEE Conference on Sensors (Sensors 2012)*, Taipei, Taiwan, Oct. 2012, pp. 2184-2187.
- [10] R.C. Roberts, and N.C. Tien, "Hexanethiol Encapsulated Gold Nanoparticle Ink For Printed Metal MEMS," *Technologies for Future Micro-Nano Manufacturing (MFG2011)*, August 8-10, 2011, Napa, Ca.
- [11] S.S. Mohan, M. Hershenson, S.P. Boyd and T.H. Lee, Simple Accurate Expressions for Planar Spiral Inductances *IEEE J. of Solid-State Circuits*, Oct. 1999, pp. 1419-24.
- [12] H.L. Krauss, C.W. Bostian, and F.H. Raad, *Solid State Radio Engineering*. New York: John Wiley & Sons, 1980. pg 76

CONTACT

*R.C. Roberts, tel: +852-28598052; rcr8@hku.hk